Toward measurements of the speed-dependence of line-mixing

Christian Boulet, Jean-Michel Hartmann

Toward measurements of the speed-dependence of line-mixing

Christian Boulet[a], Jean-Michel Hartmann[b, #]
[a]Institut des Sciences Moléculaires d'Orsay, CNRS, Université Paris-Saclay, Orsay F-91405, France.
[b]Laboratoire de Météorologie Dynamique/IPSL, CNRS, École polytechnique, Institut polytechnique de Paris, Sorbonne Université, École normale supérieure, PSL Research University, F-91120 Palaiseau, France.
[#]Corresponding author: jean-michel.hartmann@lmd.ipsl.fr

Abstract

We theoretically demonstrate that some doublets of NH_3 broadened by Ar and heavier atoms may be suitable for the first experimental demonstration of a so-far unstudied problem: The spectral effects of the speed dependence of line-mixing. By using realistic assumptions and spectroscopic data from previous studies, we show that neglecting this process leads to errors on the spectral shape of up to 2% of the peak absorption value. When multispectrum fits are made assuming speed-independent line couplings, the peak-to-dip residuals amplitudes reduce to about 0.5% and 1% for NH_3-Ar and -Xe, respectively. The magnitude of the effect is thus comparable to that of the speed dependence of the line broadening on isolated shapes, which has been demonstrated in many experimental studies. It should hence be detectable with high accuracy modern laboratory spectroscopic techniques. With this aim, guidelines and conditions paving the path for future experiments are given.

Keywords: speed-dependent line mixing, NH3 doublets, hard collision model

1. Introduction

It is now well established that the speed dependences (SD) of the pressure-broadening and -shifting coefficients must be taken into account for accurate predictions of the absorption shape of isolated lines of molecular gases [1,2]. Thanks to the unprecedented scrutiny of modern experimental techniques, many recent studies have evidenced them through fits of measured spectra using various phenomenological models, as reviewed in Sec. 4.1 of [2]. Ab initio theoretical approaches have also been proposed (e.g. [3-6]) which enable predictions of non-Voigt effects (including the influences of both the speed dependences and the collision-induced velocity changes) on the profiles of collisionally-isolated lines with a typical accuracy of a few 0.1% (e.g. [4,7-10]). Concerning the line-mixing (LM) process, its effects on spectra have been experimentally and theoretically studied for decades [1,2]. As it is now well known, they appear, in particular, in clusters of (closely spaced) overlapping pressure-broadened transitions (doublets, manifolds, Q branches). Despite the availability of several theoretical models [1,2], no prediction of the SD of LM and of its spectral consequences has been made so far. From the experimental point of view, the situation is the same: All studies in which LM parameters have been deduced from measured spectra have disregarded their speed dependence, even though the SD of the pressure-broadening and shifting coefficients were included in the fitting model (e.g. [2,11-14] and those cited therein).

The main reasons why the SD of LM has not been evidenced experimentally yet are twofold. The first one is that its influence on spectra is likely small, since it is reasonable to expect it to be comparable to that of the SD of the collisional broadening (typically 1%). The second reason is that there are few absorption features well suited for such a study and finding proper ones is not easy. Indeed, in regions involving many collisionally-coupled lines, retrieving speed-dependent LM parameters together with the numerous others (line positions

and integrated intensities, pressure-broadening and -shifting coefficients with their dependences on speed, Dicke narrowing velocity changing rate) required to describe the overall absorption is extremely difficult, if not hopeless, due to the large number of floated parameters and the subsequent correlation between them.

In the following, we theoretically show that some NH_3 doublets may be suitable for the experimental demonstration of the influence of the speed dependence of LM. The choice of the gas mixture and spectral structure is explained in Sec. 2. Then the spectral shape model and data used for the spectra simulations are described in Sec. 3, the spectra simulations and their fitting procedure being detailed in Sec. 4. The results obtained in the test case of the $^{p}P(6,6)$ doublet of NH_3 are presented and discussed in Sec. 5 where the sensitivity of the results to various parameters is studied. The cases of other doublets are discussed in Sec. 6 where some advices for experiments are also given, before providing conclusive remarks in Sec. 7.

2. Choosing the gas mixture and spectral structure

Our search for spectral structures suitable for the experimental demonstration of the speed dependence of LM was constrained by the following criteria.

(i) The retained transitions should show strong LM effects at properly chosen pressures. This implies that the involved relaxation matrix elements at pressure *P*: $|\bar{W}_{\ell,\ell'}| = \left\langle |W_{\ell,\ell'}(v)| \right\rangle = P\left\langle |w_{\ell,\ell'}(v)| \right\rangle$, where <…> denotes an average over the speed *v* of the absorbing molecule while ℓ and ℓ' designate the collisionally-coupled lines, should be significant when compared to the speed-averaged pressure-broadened half width $\bar{\Gamma}_\ell = \left\langle \Gamma_\ell(v) \right\rangle = P\left\langle \gamma_\ell(v) \right\rangle$. This is an obvious prerequisite for the influence of the SD of LM to be as detectable as possible, since the strongest effects are expected when the influence of LM is the largest. Note that, as discussed later, other criteria condition the choice of the collision partner through the absorber-perturber interaction potential and mass ratio.

(ii) The number of significantly coupled lines should be as small as possible, ideally no more than two. This ensures that the number of floated parameters in the fits of measured spectra is small enough to limit the potential ambiguity and bias of the results induced by correlations between the unknowns.

(iii) The distances $\Delta\sigma_{\ell,\ell'}=|\sigma_\ell - \sigma_{\ell'}|$ between the collisionally-coupled lines should be sufficiently large to have, for *some* (but not all) total pressures *P*, a pressure broadened width $\bar{\Gamma}_\ell = P\left\langle \gamma_\ell(v) \right\rangle$ much larger than the Doppler width (Γ_D) , i.e. $P >> \Gamma_D / \left\langle \gamma_\ell(v) \right\rangle$, while keeping a weak overlapping, i.e. $\bar{\Gamma}_\ell << \Delta\sigma_{\ell,\ell'}$ and thus $P << \Delta\sigma_{\ell,\ell'} / \left\langle \gamma_\ell(v) \right\rangle$. This enables to limit the potential effects of the above mentioned correlations by ensuring that the parameters describing the isolated line-shapes (unperturbed positions, integrated intensities, speed-dependent widths and shifts, Dicke narrowing) can be constrained under weak LM conditions.

(iv) In addition, the values of $\Delta\sigma_{\ell,\ell'}$ should also be sufficiently small to enable a strong overlapping, i.e. $P\left\langle \gamma_\ell(v) \right\rangle >> \Delta\sigma_{\ell,\ell'}$, and thus large LM effects, for *some* (but not all) pressures that can be investigated with current laboratory set ups. This criterion complements (iii) without contradicting it since the adapted pressure ranges mentioned are different for the two criteria.

(v) The contribution of "perturbing" lines, either weak ones lying very close to those of interest or strong ones on the sides on the targeted spectral interval, should be as small as possible. This ensures that uncertainties in the modeling of these “undesirable” absorptions,

which do not carry accessible information on the SD of LM, do not pollute and bias the results too much.

An extensive bibliography search based on the above criteria shows that, among the spectral structures for which data on line-broadening and (speed independent) LM are available from previous studies, some NH_3 doublets (see Sec. 3.2) are good candidates, if not the best ones. The latter, as well as isolated NH_3 lines, were investigated in several experimental and theoretical studies ([15-20] and those therein). Although speed-independent LM or isolated-line fitting models were used in these studies, the latter provide starting data for the present investigation.

Considering the collision partners, one should retain those for which large speed dependences of the LM parameters are expected. For their selection, we consider the law derived [21] for the SD of the broadening by assuming resonant collisions (i.e. that collision-induced rotational energy changes are very small when compared with the translational energy) and a absorber-perturber interaction potential dominated by terms proportional to $1/R^q$, where R is the intermolecular distance. The evolution of the broadening coefficient $\gamma(v)$ with the absorber speed is then proportional to the confluent hypergeometric function $M[-(q-3)/(2q-2),3/2,-\Lambda v^2/\tilde{v}^2]$, where $\tilde{v}=\sqrt{2k_BT/m}$ is the most probable absorber speed and $\Lambda = m_p/m$ is the ratio of the perturber and absorber masses. The relative magnitude of the speed dependence can be evaluated by considering $R(q,\Lambda)=[\gamma(v_+)-\gamma(v_-)]/\gamma(\tilde{v})$, which quantifies the variations of the broadening between speeds v_- and v_+, relative to the value for $\tilde{v}$. Retaining $v_- \approx 0.38\tilde{v}$ and $v_+ \approx 1.81\tilde{v}$, which are representative in terms of the thermal Boltzmann distribution since $v_-^2 \exp(-v_-^2/\tilde{v}^2) = v_+^2 \exp(-v_+^2/\tilde{v}^2) = \tilde{v}^2 \exp(-\tilde{v}^2/\tilde{v}^2)/3$, and using:

$$R(q,\Lambda)=\frac{M[-(q-3)/(2q-2),3/2,-\Lambda v_+^2/\tilde{v}^2]-M[-(q-3)/(2q-2),3/2,-\Lambda v_-^2/\tilde{v}^2]}{M[-(q-3)/(2q-2),3/2,-\Lambda\tilde{v}^2/\tilde{v}^2]}, \quad (1)$$

lead to the results displayed in Fig. 1 for various values of q and Λ.

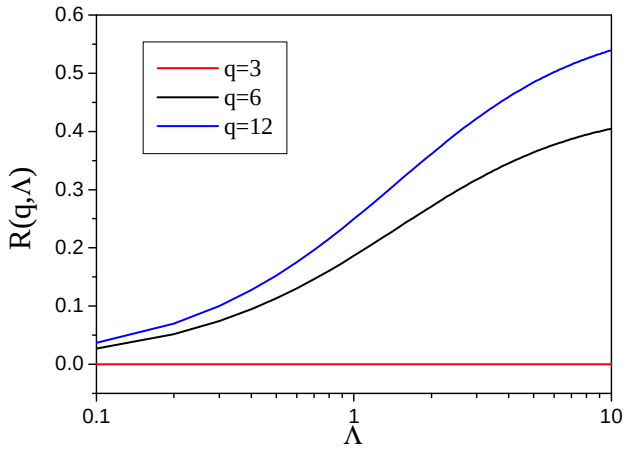

Fig. 1: Relative variation $R(q,\Lambda)$ (see text) of the hypergeometric speed dependence versus the ratio Λ of the perturber and absorber masses for different powers q of the intermolecular potential.

As can be seen and is well known, the pressure broadening is speed independent for q=3, which is associated with strong dipole-dipole interactions, since $M[0,3/2,-\Lambda v^2/\tilde{v}^2]$=1. This implies that pure NH_3 should be disregarded despite the fact that strong (but thus speed independent) LM effects affect some doublets [15, 18, 20, 22]. Relatively light perturbers, for which $\Lambda << 1$ and $R(q,\Lambda)$ is small, are also poor candidates for the present study. This rules out NH_3-H_2 although strong (but again weakly speed-dependent) couplings exist within doublets [15]. Note that these predicted weak speed dependences of the line broadenings for pure NH_3 and NH_3-H_2 are confirmed by the small values of the quadratic-law parameter $\Delta\gamma/\gamma$ [see Eq. (8)] obtained from fits of measured spectra in [17]. Finally, Fig. 1 shows that large values of both q and Λ are favorable, making relatively heavy ($\Lambda >> 1$) and non polar (with intermolecular potentials dominated by dispersion forces with $q \approx 6$) perturbers the best candidates. Adding the further restriction that data on the speed-dependent broadening and speed-independent LM should be available in the literature for the finally retained system leads to argon as the first choice for the NH_3 collision partner.

3. Spectral shape model and data used

3.1 Spectral shape

The spectral shape model used here is that proposed in [23] which assumes uncorrelated hard collisions, i.e.: that the changes of the translational and rotational motions are uncorrelated and that collisions thermalize the translational speed. The frequency $f(v' \leftarrow v)$ of changes from a translational speed v to v' is then independent of v and given by $f(v' \leftarrow v)=Bf_{MB}(v')$, where $f_{MB}(v')$ is the Maxwell-Boltzmann factor and $B = P\beta$ is the (speed independent) velocity-changing collision rate. Recall that, for collisionally-isolated lines, complementing this model with speed-dependent widths and shift leads to the so-called speed-dependent Rautian (or Nelkin-Ghatak) profile [1]. The latter, as well as the (equivalent) un-correlated Hartmann-Tran profile [24,25] which assumes quadratic speed dependences, have enabled very accurate fits of measured and calculated isolated line shapes for a variety of absorber-perturber pairs (e.g. references in Sec. 4.1 of [2]). The absorption coefficient $\alpha(\omega)$ at angular frequency $\omega = 2\pi c\sigma$, σ being the wave number, is then given by Eqs. (2.14) and (3.1) of [23]:

$$\alpha(\omega) = N_a \frac{4\pi^2\omega}{3\hbar c}\left[1-\exp(\hbar\omega/k_B T)\right]\tilde{\alpha}(\omega) \ , \qquad (2)$$

where N_a is the number density of absorbing molecules, and:

$$\tilde{\alpha}(\omega) = \frac{1}{\pi}\mathrm{Re}\left\{\boldsymbol{\mu}^t.\left[\mathbf{Id} - B\mathbf{G}(\omega)\right]^{-1}.\mathbf{G}(\omega).\boldsymbol{\rho}_0.\boldsymbol{\mu}\right\} \ . \qquad (3)$$

In this expression, $\mathbf{Id}$ denotes the unity matrix, $\boldsymbol{\mu}$ is a column vector ($\boldsymbol{\mu}^t$ being its transpose) of the dipole transition moments in the (Liouville) line space, and $\boldsymbol{\rho}_0$ is the diagonal matrix of the populations of the initial levels of the lines. The matrix $\mathbf{G}(\omega)$ is obtained from its speed-dependent equivalent $\mathbf{G}(\omega, v)$:

$$\mathbf{G}(\omega,\vec{v}) = \left[\ \mathbf{W}(v) + B\mathbf{Id} - i(\omega\mathbf{Id} - \boldsymbol{\Omega}_0 - \vec{k}.\vec{v}\mathbf{Id})\right]^{-1} \ , \qquad (4)$$

through the equilibrium average:

$$\mathbf{G}(\omega) = \int \mathbf{G}(\omega,\vec{v}) f_{MB}(v) d^3\vec{v} \ . \qquad (5)$$

In Eq. (4), $\mathbf{\Omega}_0$ is the diagonal matrix of the unperturbed line positions ω_ℓ, $\vec{k}$ is the radiation wave vector (the term $\vec{k}.\vec{v}$ leading to the Doppler effect), and $\mathbf{W}(v)$ is the speed-dependent impact (thus frequency independent) relaxation matrix in the line space. The diagonal elements of $\mathbf{W}(v)$ are the pressure-induced width $\Gamma_\ell(v)$ and spectral shift $\Delta_\ell(v)$ of the individual transitions, with:

$$\mathbf{W}_{\ell,\ell}(v) = \Gamma_\ell(v) + \mathrm{i}\Delta_\ell(v) \ , \tag{6}$$

while the off-diagonal elements $\mathbf{W}_{\ell,\ell'}(v)$, which describe the coupling between lines ℓ and ℓ', are responsible for the line mixing process. In general, the preceding equations, which involve matrix inversions, must be solved numerically, but, as shown in [23], much can be done analytically in the case of a doublet, thanks to the fact all matrices have 2 by 2 dimensions.

3.2 Data used

First recall that, within the binary collisions approximation, valid at the pressures considered below, all collisional parameters are proportional to the gas density (i.e. that of the collision partner for highly diluted absorbing molecules). Assuming an ideal gas, one can thus write $\Gamma_\ell(v) = P\gamma_\ell(v)$, $\Delta_\ell(v) = P\delta_\ell(v)$, $\mathbf{W}_{\ell,\ell'}(v) = P\mathbf{w}_{\ell,\ell'}(v)$, and $\mathrm{B} = P\beta$ where all lower case letters are pressure normalized and expressed in rad/s/atm (cm^{-1}/atm if wave numbers are used).

Concerning the speed dependences of the widths and shifts, they are commonly described using two different approaches. The first is the hypergeometric function [21] introduced at the end of Sec. 2, i.e. (with $\Lambda = m_p / m$):

$$(\gamma \text{ or } \delta)(v) = (\overline{\gamma} \text{ or } \overline{\delta}) \times (1+\Lambda)^{-\frac{q-3}{2q-2}} M\left(-\frac{q-3}{2q-2}, \frac{3}{2}, -\Lambda\frac{v^2}{\tilde{v}^2}\right) . \tag{7}$$

The second approach assumes a quadratic dependence [26], i.e.:

$$(\gamma \text{ or } \delta)(v) = (\overline{\gamma} \text{ or } \overline{\delta}) \times \left[1 + \left(\frac{\Delta\gamma}{\overline{\gamma}} \text{ or } \frac{\Delta\delta}{\overline{\delta}}\right) \times (v^2/\tilde{v}^2 - 3/2)\right] . \tag{8}$$

Note that q, or alternatively $\Delta\gamma/\overline{\gamma}$ and $\Delta\delta/\delta$, are quantities that are generally floated, together with $\overline{\gamma}$ and $\overline{\delta}$, while carrying fits of measured speed-dependent line shapes (e.g. Sec. 4.1 of [2] and, for NH_3, Ref. [17]).

By consistency with these approaches for the broadening and shifting, and in the absence of any alternative model, the same equations are used here for the speed dependences of the line coupling terms $\mathbf{w}_{\ell,\ell'}(v)$, which were, in addition, considered purely real-valued since nothing is known on their expected very small imaginary part. In other words, we use the same value of q for all the collisional parameters [i.e. for $\gamma_\ell(v)$, $\delta_\ell(v)$ and $w_{\ell\ell'}(v)$]. This is (partly) justified by the fact that the rotational state changes between the levels of the selected doublet transitions, responsible for $\mathbf{w}_{1,2}(v)$ and $\mathbf{w}_{2,1}(v)$, make a large contribution to the broadening coefficients $\gamma_1(v)$ and $\gamma_2(v)$, as shown by Table 1.

As explained in Sec. 2, we have retained NH_3 doublets perturbed by Ar since they are, in our opinion, the best candidates for the demonstration of the SD of LM. Among them the $^{P}P(6,6)$ of the ν_4 band and the $^{R}R(4,4)$ of the ν_3 band are of particular interest because their two transitions are significantly coupled and relatively little affected by perturbing lines. Furthermore, these two doublets are in different regions (6.53 and 2.85 μm, respectively),

which provides flexibility for measurements. Within the above mentioned choices, Table 1 summarizes the data used, which were obtained as follows: The unperturbed line positions $\sigma_{1,2}$ and the integrated intensities $S_{1,2}(296\text{K})$ of the two lines (subscripts 1 and 2) were taken from the 2016 edition of the HITRAN database [27]. Note that the dipole transition moments $\mu_{1,2}$ for Eq. (3) can be deduced from the latter through:

$$S_{1,2}(T) = (8\pi^3\sigma_{1,2}/3\hbar)\left[1-\exp(hc\sigma_{1,2}/k_{\text{B}}T)\right]\rho_0(T)_{1,2}\mu_{1,2}^2 \ , \qquad (9)$$

where $\rho_0(T)_\ell$ is the relative population of the lower level of line ℓ. The speed-averaged pressure broadening coefficients $\overline{\gamma}_{1,2}$ were assumed equal (a good approximation) with values $(\overline{\gamma}_1+\overline{\gamma}_2)/2$ deduced from those given in [15] and [19] for the transitions of the ν_4 and ν_3 bands, respectively. The same two references provided the relaxation matrix elements $\overline{w}=\overline{w}_{12}=\overline{w}_{21}$ (since ρ_1 and ρ_2 have extremely close values) coupling the two lines. Note that, in the absence of measurements for the $^{\text{R}}$R(4,4) doublet, the theoretical prediction of $\overline{w}$ from [19] was empirically corrected using $\overline{w}[^{\text{R}}\text{R(4,4)}]=\overline{w}^{\text{calc}}[^{\text{R}}\text{R(4,4)}]\times\left\{\overline{w}^{\text{meas}}[^{\text{P}}\text{P(5,5)}]/\overline{w}^{\text{calc}}[^{\text{P}}\text{P(5,5)}]\right\}$, where the superscripts "calc" and "meas" denote values from Refs. [19] and [15], respectively. The line shifts were disregarded in a first step, but the sensitivity of the results to these parameters is discussed later. For the hypergeometric model, the parameter q driving the speed dependences through Eq. (7) [which also applies to $w_{12}(v)$ and $w_{21}(v)$] was taken equal to 6. This value, which assumes that dispersion forces in R^{-6} dominate the NH_3-Ar interaction, is consistent with those deduced from measured spectra in [17]. Similarly, the velocity changing rate β=0.02 cm^{-1}/atm is representative of those given in [17].

Parameters	$^{\text{P}}$P(6,6) ν_4 band	$^{\text{R}}$R(4,4) ν_3 band
σ_1 (cm^{-1})	1532.4503	3505.4364
σ_2 (cm^{-1})	1532.6830	3505.8700
$S_1 = S_2$ (cm^{-2}/atm)	1.209	0.0653
$\overline{\gamma}=\overline{\gamma}_1=\overline{\gamma}_2$ (cm^{-1}/atm)	0.0494	0.0496
$\overline{\delta}_1=\overline{\delta}_2$ (cm^{-1}/atm)	0	0
$\overline{w}=\overline{w}_{12}=\overline{w}_{21}$ (cm^{-1}/atm)	-0.018	-0.019
β (cm^{-1}/atm)	0.02	0.02
$q=q_\gamma=q_w$	6	6

Table 1: Spectroscopic and collisional parameters used for the calculation of the shapes of Ar-broadened NH_3 doublets.

4. Spectra simulations and their fitting procedure

4.1 Simulating the spectra

In a first step, spectra for each doublet (with lines denoted as 1 and 2) were calculated at various pressures $P_{i=1,n}$ using the equations and values of the spectroscopic parameters given above. The pressure range was chosen in order to span the various collisional regimes, thus including:

(i) “Small” pressures for which line mixing effects are negligible, i.e. such that $P\overline{\gamma}_{1,2} << |\sigma_1 - \sigma_2|$, while the shapes of the lines show a significant Doppler effect and Dicke narrowing, i.e. for $P\overline{\gamma}_{1,2}/\Gamma_D$ of the order of unity or smaller.

(ii) “Intermediate” P values for which line mixing effects are still negligible, i.e. such that $P\overline{\gamma}_{1,2} << |\sigma_1 - \sigma_2|$, while the shapes of the lines are now dominated by the collisional broadening, i.e. $P\overline{\gamma}_{1,2}/\Gamma_D >> 1$.

(iii) “Large” pressures for which collisional line-mixing significantly influences the overall absorption profile, such that $P\overline{\gamma}_{1,2}/|\sigma_1 - \sigma_2|$ is of the order of unity or greater.

The spectra simulated in such a way show effects of velocity changes (Dicke narrowing, through β), of the pressure broadening, through $\overline{\gamma}_{1,2}$, and of its speed dependences, through q_γ, of line mixing, through $\overline{w}_{12}$ and $\overline{w}_{21}$ as well as of their speed dependence, through q_w. Note that the relative importance of each of the above mentioned collisional effects depends on the pressure, as discussed below.

The spectra calculated for the ^{P}P(6,6) doublet using the data of Table 1 and the equations in Sec. 3.1 are shown in the main panel of Fig. 2. The insert displays the ratios $P\overline{\gamma}/\gamma_D$ and $P\overline{\gamma}/|\Delta\sigma_{12}|$ showing that the three pressure regimes discussed above are indeed included in the 20-4000 Torr range retained. One can schematically say that the two lowest pressures essentially provide information on velocity changes and on the Dicke narrowing process (i.e. on β). For the three next pressures, the pressure broadening and its speed dependence (i.e. $\overline{\gamma}$ and q_γ) play an increasing role while the line overlapping is still small and LM effects are weak. Then, the latter (i.e. $\overline{w}$ and q_w) have a significant influence and change the absorption more and more at the three highest pressures. For 4000 Torr and above, the doublet starts to look like a single line. In this case of strong overlapping, its profile is essentially governed by the effective broadening coefficient $\overline{\gamma} + \overline{w}$ and the associated speed dependences, as shown in Sec. IV.2.2b of [1]. This is when the relative influence of LM, and thus also of its SD, is the greatest, as demonstrated by Fig. 3. This figure also shows that neglecting the SD of LM then leads to an underestimation of the doublet width, with errors on the absorption of typically 1% of the peak value that have a M shape. This could be expected (recalling that $\overline{w}_{12}$ and $\overline{w}_{21}$ have negative values) from the well known fact ([1,2], and [17] for NH_3) that the speed dependence of the broadening results, for isolated lines, in a narrowing with changes of the absorption of similar magnitudes and a W shape (a M shape if transmissions are considered).

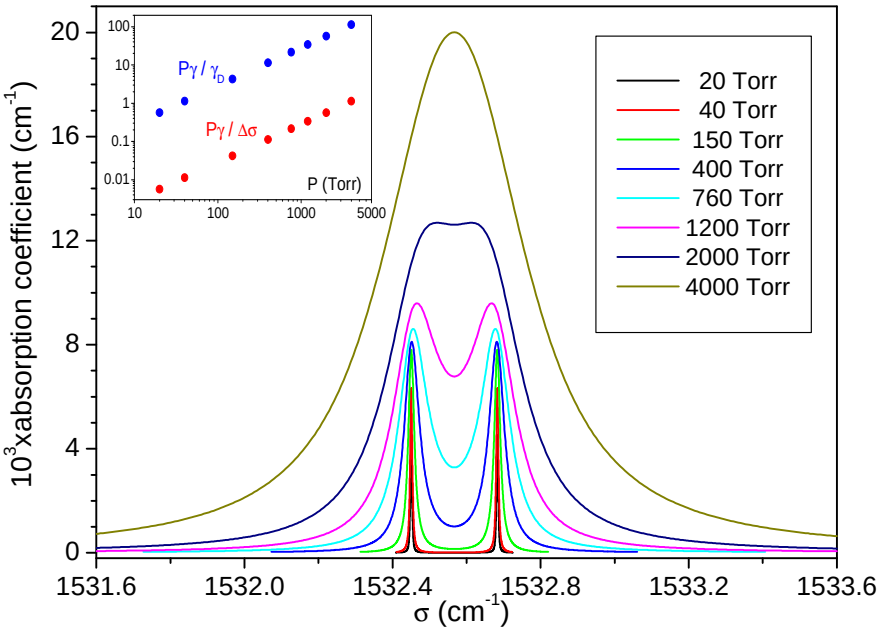

Fig. 2: Absorption coefficients calculated, for the ^{P}P(6,6) doublet (alone) for 0.1% NH_3 diluted in Ar at various pressures, using the hypergeometric speed-dependence law. The insert displays the variations of the ratio of the pressure broadened and Doppler half widths, denoted $P\gamma/\gamma_D$, and that of the pressure broadened half width and line separation, denoted $P\gamma/\Delta\sigma$.

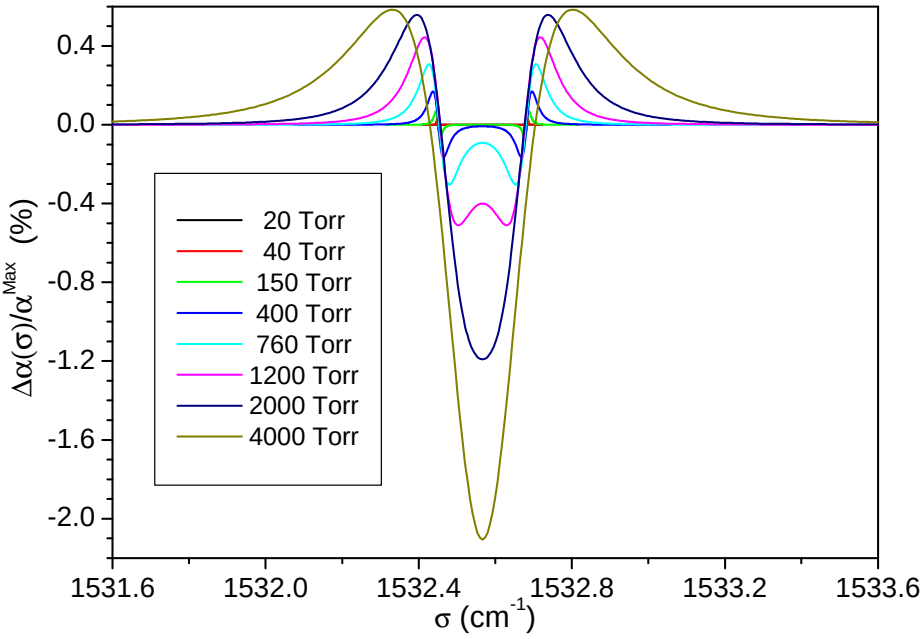

Fig. 3: Differences between the absorptions computed, for the ^{P}P(6,6) doublet (alone) for 0.1% NH_3 diluted in Ar at various pressures, using the parameters of Table 1 with (thus using q_w =6) and without (thus using q_w =3) the inclusion of the speed dependence of line mixing, relative the peak absorption value.

4.2 Fitting procedure

In a second step, which leads to the various results presented in Sec. 5, the spectra simulated for each doublet at various pressures (20-4000 Torr, e.g. Fig. 2) as explained above, were simultaneously adjusted using a multispectrum fitting procedure [28] with a model that neglects the SD of LM. In other words, σ_1 , σ_2 , S_1 , S_2 , $\overline{\gamma} = \overline{\gamma}_1 = \overline{\gamma}_2$, q_γ (or $\Delta\gamma_1 / \overline{\gamma} = \Delta\gamma_2 / \overline{\gamma}$), and $\overline{w} = \overline{w}_{12} = \overline{w}_{21}$ were floated while q_w =3 (or $\Delta w / \overline{w}$ =0) was imposed. The root-mean square of the deviation between the input and fitted absorption coefficients, including all spectral points at the 8 pressures in Fig. 2, was minimized. Note that the Doppler width was fixed to its input value, and that no baseline was floated in the fits.

5. Results for the test case of the ^{P}P(6,6) doublet of NH_3 in Ar

5.1 Hypergeometric/Hypergeometric

As a first exercise, we adjusted the spectra of Fig. 2, simulated for the ^{P}P(6,6) doublet using the parameters of Table 1 with the hypergeometric law, by using exactly the same model and floating all parameters. The fact that the obtained parameters and fitted spectra are exactly identical to the input ones, as they should be since the spectra carry no noise, validates the numerical procedure.

Then, the same model, but now disregarding the speed dependence of line-mixing (i.e. fixing the value of q_w to 3) was used in the fits. Table 2 (columns 2 and 3) provides a comparison between the input and retrieved (fitted) collisional parameters. As can be seen, there is a good agreement, with small differences that can be explained by the above mentioned fact that the SD of LM induces a broadening of the absorption feature when the two lines overlap significantly. Indeed, the fit without the SD of LM tries to mimic this through the adjustment of $\overline{\gamma}$, q_γ , and $\overline{w}$ by: increasing $\overline{\gamma} + \overline{w}$ and decreasing q_γ , two changes that both contribute to a broadening of the absorption structure at elevated pressure.

Parameter	Input Hypergeo	Fitted Hypergeo	Fitted quadratic
σ_1 (cm^{-1})	1532.4503	1532.4503	1532.4503
σ_2 (cm^{-1})	1532.6830	1532.6830	1532.6830
$S_1 = S_2$ (cm^{-2} atm^{-1})	1.209	1.209	1.209
$\overline{\gamma} = \overline{\gamma}_1 = \overline{\gamma}_2$ (cm^{-1} atm^{-1})	0.0494	0.0490	0.0491
q_γ	6.0	4.8	
$\Delta\gamma / \overline{\gamma}$			0.123
$\overline{\delta}_1 = \overline{\delta}_2$ (cm^{-1} atm^{-1})	0.	0. (fixed)	0. (fixed)
$\overline{w} = \overline{w}_{12} = \overline{w}_{21}$ (cm^{-1} atm^{-1})	-0.0180	-0.0174	-0.0174
q_w	6.0	3.0 (fixed)	
$\Delta w / \overline{w}$			0.0 (fixed)
β (cm^{-1} atm^{-1})	0.020	0.0238	0.0248

Table 2: Input and fitted parameters for the ^{P}P(6,6) doublet broadened by Ar.

The fit residuals, shown in Fig. 4 (see also Fig. 5), call for the following remarks. The first is that their amplitudes are, when compared to those in Fig. 3, significantly reduced at the

elevated pressures and increased at the lowest ones with sign changes in some cases. This results from the adaptation of the parameters (leading to ad-hoc but "wrong" values of $\overline{\gamma}$, q_γ, β and $\overline{w}$, see Table 2) made by the multispectrum fit in order to adjust, as well as possible, all the input data. Furthermore, detailed analysis demonstrates that the pressure-dependent shapes of the fit residuals can be explained by the differences between the input and fitted parameters displayed in Table 2. Finally recall that the shapes and magnitudes of the residuals depend on the weight associated with each spectrum. Different results may thus be obtained if, for instance, the high (resp. low) pressure spectra included less (resp. more) spectral points, as discussed latter.

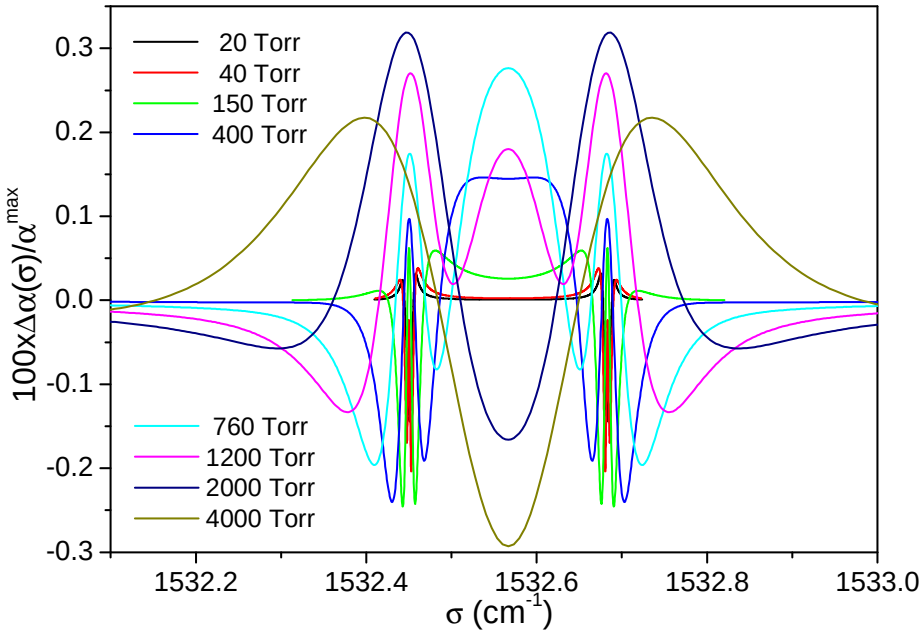

Fig. 4: Differences, relative the peak absorption value, between the input absorptions (Fig. 2) computed for the ^{P}P(6,6) doublet (alone) for 0.1% NH_3 diluted in Ar at various pressures, and the fitted results without (q_w =3) the inclusion of the speed dependence of line mixing.

5.2 Hypergeometric/Quadratic

In order to evaluate the influence of the use of an approximate speed-dependence model (which is the case for both the hypergeometric and quadratic laws), the same spectra, simulated using the hypergeometric law, were refitted using a quadratic speed-dependent broadening [Eq. (8)], still disregarding the SD of LM. The obtained values are displayed in Table 2 (column 4) where they can be compared with the input ones (column 2). The comments made above for the fit using the hypergeometric law and concerning columns 2 and 3 of Table 2 remain valid. Furthermore, the fit residuals (not shown) are very similar to those displayed in Fig. 4 with peak-to-dip amplitudes relative to the maximum absorption value also close to 0.5% when LM effects are significant, as shown by Fig. 5. The only significant differences appear at low pressures and result for the differences (quadratic instead of hypergeometric) in the modelling of the speed dependence of the broadening.

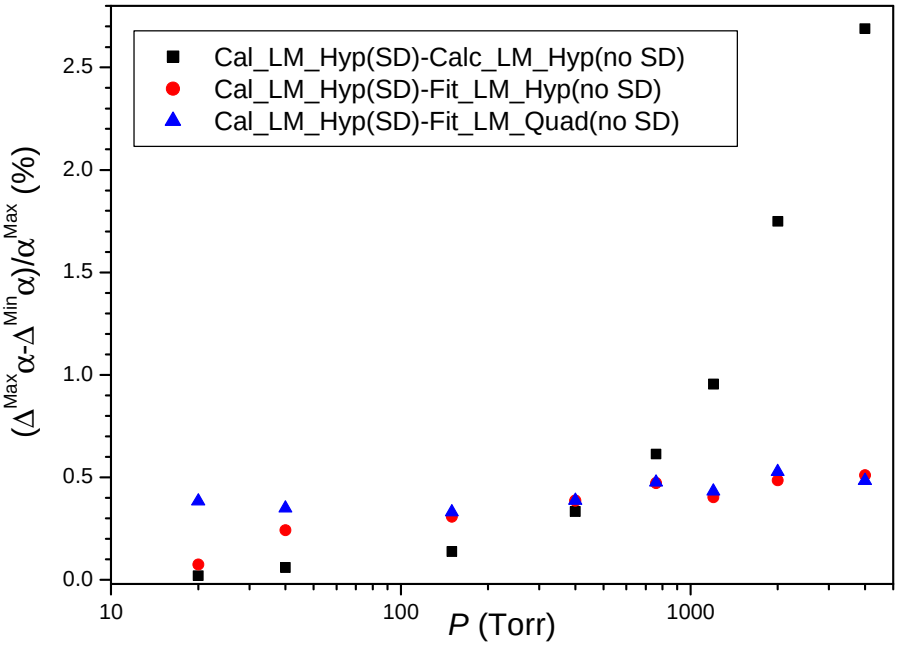

Fig. 5: Peak-to-dip amplitudes of differences between spectra of the ^{P}P(6,6) doublet (alone) for 0.1% NH_3 diluted in Ar , relative to the peak absorption values. The reference spectrum is that computed with the parameters of Table 1 and differences are shown with those: computed with the same parameters but disregarding the SD of LM (black squares) ; fitted using the hypergeometric speed dependence with no SD of LM (red circles) ; fitted using the quadratic speed dependence with no SD of LM (blue triangles).

5.3 Influences of other collisional parameters

We here investigate the influence of changes of some input collisional parameters on the results obtained for spectra simulated and adjusted using the hypergeometric law, still disregarding the SD of LM in the fits.

● *Influence of the pressure shift*: Here, ^{P}P(6,6) spectra were first simulated using the parameters in Table 1 complemented by line shifts that were equal for the two lines ($\overline{\delta}_1 = \overline{\delta}_2 = 4\ 10^{-3}$ cm^{-1}/atm according to the predictions in [16]). Multispectrum fits disregarding the SD of LM were then made by floating $\overline{\delta}$ together with the other parameters (as done above), while imposing a consistent constraint (i.e. $\overline{\delta}_1 = \overline{\delta}_2 = \overline{\delta}$). The results show that the value of $\overline{\delta}$ is very well retrieved and that the fit-residuals and the values of the other parameters are practically identical to those obtained (Sec. 5.1) when all shifts are disregarded. This could be expected since the fitted spectral structures are fully symmetric (with respect to the doublet center) and because $\overline{\delta}$ only induces an overall displacement of the absorption spectra without affecting their shapes. A second exercise was carried, in which spectra simulated without any shift were adjusted floating shifts of opposite signs (i.e. $\overline{\delta}_1 = -\overline{\delta}_2$). It provides a more stringent test because it has been shown that shifts of opposite signs may mimic LM effects [15,29] by "wrongly" making the two lines closer in order to increase the absorption at the center and reduce it in the wings on both sides. Again, and thanks to the fact that spectra in a broad range of pressure are simultaneously fitted, the changes of the retrieved parameters and fit residuals are very small. This demonstrates that introducing shifts in the fits does not affect the detectability of the influence of the SD of LM.

● *Influence of the narrowing parameter*: In order to quantify the influence of the frequency of velocity changing collisions, the hypergeometric/hypergeometric study of Sec. 5.1 was redone with the input value of β changed by factors of 1/2 and 2, leading to the results displayed in Fig. 6. As can be seen (compare full back squares, full blue and red circles), increasing β reduces the residuals. This could be expected since large values of β favor exchanges between the various speed classes, and thus leads to a reduction of the inhomogeneous effects tied to the speed dependences of both the broadening and line mixing.

● *Influence of the perturber (mass)*: In order to quantify the influence of the mass of the collision partner, the hypergeometric/hypergeometric study of Sec. 5.1 was redone replacing Ar (40 g) by Kr (84 g) and Xe (131 g). With respect to those for Ar, slightly different input values of $\overline{\gamma}$, $\overline{w}$ and β were used, increased by about 10% for Kr and 28% for Xe. In the absence of experimental values, these changes for $\overline{\gamma}$ (thus also applied to $\overline{w}$) and β were estimated, assuming a dominant dipole-induced dipole (in R^{-6}) absorber-perturber interaction, from the changes of the mass and isotropic polarizability of the collision partner. Figure 6 shows (compare full black squares, down cyan and magenta triangles), consistently with the results in Fig. 1, that the residuals are the largest when the perturber mass is the highest, in agreement with studies for isolated lines (e.g. [11,17,30-33]).

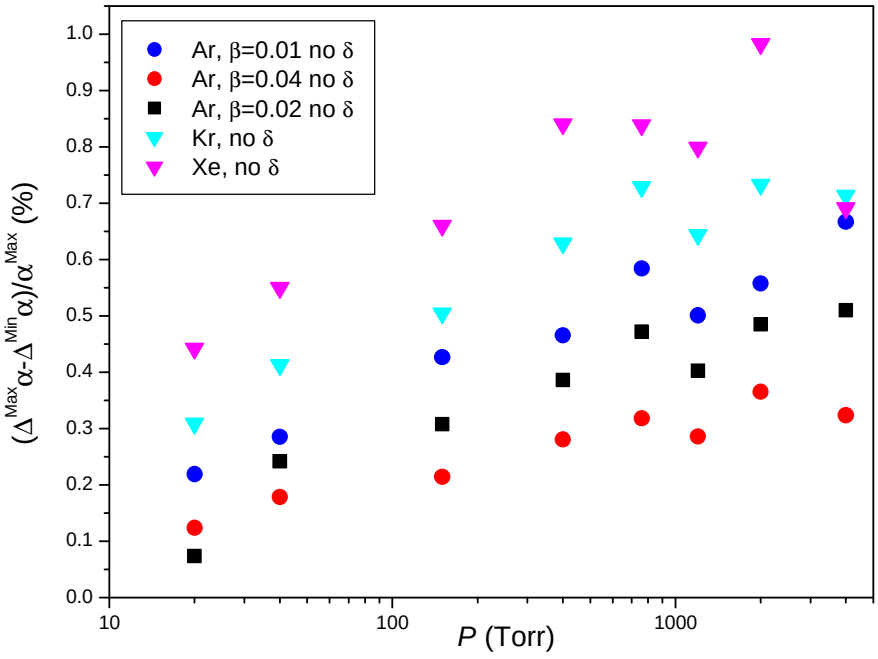

Fig. 6: Influences of the narrowing parameter, perturber mass and line shift on the peak-to-dip amplitudes of the fit residuals for the ^{P}P(6,6) doublet (alone), relative to the peak absorption values. All reference spectra (and fits) have been computed using the hypergeometric speed dependence.

5.4 Influence of "perturbing" transitions.

In real NH_3 spectra, the doublets are not fully isolated, and other lines within or on the sides of the spectral region where the two lines of interest significantly absorb can contribute to the overall absorption. In order to investigate the effect of errors in the modeling of these contributions, reference spectra at the selected 8 pressures were computed by adding, to the isolated doublet absorption of Fig. 2, 5% of the absorption of the other lines (computed using

Voigt profiles). These spectra were then fitted considering that the doublet is alone (thus assuming a perfect modeling of the perturbing lines contributions and without adjustment of any baseline) and neglecting the SD of LM. This is strictly equivalent to a procedure in which the doublet is fitted while the computed (and fixed) contribution of perturbing lines carries a relative error of 5%. The changes of the residuals (with respect to those in Fig. 4) can be seen in Fig. 7. As could be expected, the approximate (5% error) computation of the absorption due to lines other than the ^{P}P(6,6) doublet modifies the residuals. However, the latter have shapes and magnitude that are not too different from those obtained when the doublet is fully isolated. In other words, the influence of the SD of LM remains distinguishable.

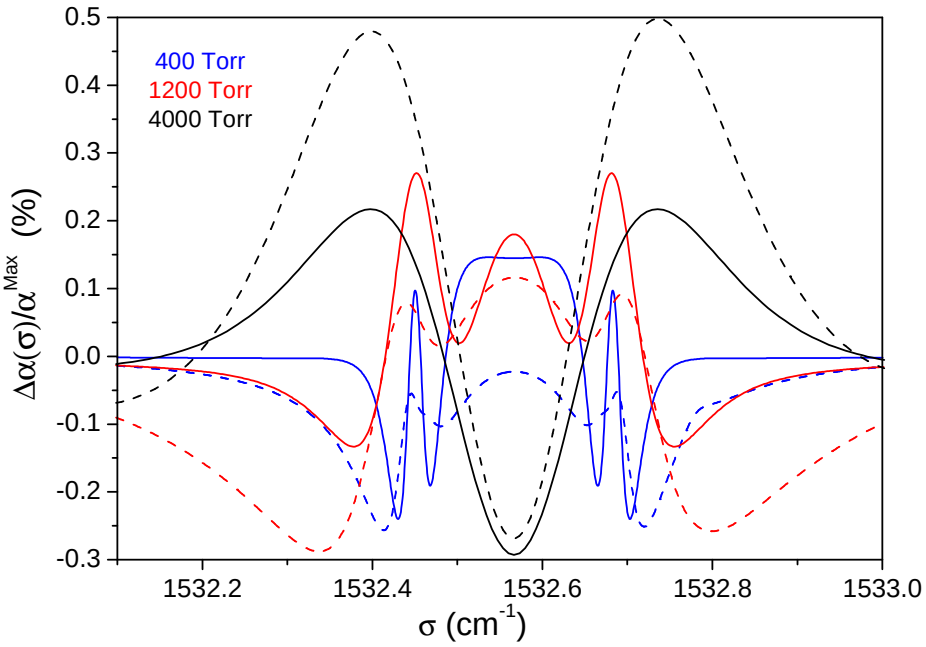

Fig. 7: Peak-to-dip amplitudes of the residuals of fits of spectra of the ^{P}P(6,6) doublet (alone) for 0.1% NH_3 diluted in Ar , relative to the peak absorption values. The full (resp. dashed) lines have been obtained disregarding (resp. taking into account) the other lines in the calculations of the references spectra while all fits disregarded this contribution.

6. Other doublets and advices for experiments

6.1 Other doublets

As mentioned above, the ν_3 band ^{R}R(4,4) doublet is another good candidate for the experimental highlighting of the speed dependence of line mixing. It offers a potentially interesting alternative to the ^{P}P(6,6) doublet of the ν_4 band because it lies in a different spectral region. Table 1 shows that the spacing between its two transitions and its Doppler width are both approximately two times larger than those of the ^{P}P(6,6) while the collisional parameters are similar. This implies that all results obtained for the ^{P}P(6,6) are directly applicable to the ^{R}R(4,4) provided that the pressure *P* is doubled. In other words, the ^{R}R(4,4) shape for a given *P* value is close to that of the ^{P}P(6,6) for *P*/2. However note that the lines intensities are about 18 times smaller which requires the use of significantly longer path lengths in the measurements.

Recall that large LM effects have been evidenced in several other doublets of the ν_4 band for NH_3 diluted in Ar [15], including the ^{P}P(5,5) and ^{P}P(7,7) for instance. Although they are

more affected by perturbing lines contributions their shapes deserve measurement and analysis, particularly if broad band spectra covering a large part of the ν_4 band are recorded (e.g. by Fourier transform).

6.2 Advices for dedicated experiment

In order to unambiguously highlight the (small, see Figs. 4 and 6) influence of the speed dependence of line mixing on the proposed NH_3 doublets, dedicated experiments should satisfy several demanding constrains. The latter, which are discussed below, also apply for studies of refined effects on the shapes of isolated lines, but extended pressure and spectral ranges must be investigated for the present study.

(i) As discussed in Sec. 1, measurements should ideally be made for a range of total pressures for which the pressure-broadened widths vary from below the Doppler width to above the doublet lines separation.

(ii) The total pressure of each studied sample should be very precisely known, with an uncertainty (0.1% or less) much smaller that the expected residuals obtained when the SD of LM is disregarded (see Fig. 5).

(iii) Mixtures in which NH_3 is highly diluted should be used for two reasons. The first is that, since the self broadening of ammonia is almost speed independent, NH_3-NH_3 collisions provide no information on the SD of LM. The second, more crucial, is that errors on the knowledge of the NH_3 relative amount $x(NH_3)$ that are inconsistent from one sample to another will bias the results. In order to define a criterion, let us target an error smaller than 0.1% on the spectral shape, assume that $x(NH_3)$ is known within a relative uncertainty of $\delta_{x(NH_3)}$, and consider the influence of the pressure broadening. The self-broadening coefficient being about ten times larger than that by Ar [15,34], one straightforwardly obtains: $10x(NH_3)\delta_{x(NH_3)} \leq 10^{-3}$. Assuming the conservative value $\delta_{x(NH_3)}$=5% (from analysis of the absorbance area for instance) then leads to $x(NH_3) \leq 0.2$ %.

(iv) Temperature variations between measurements at different total pressures should remain small. For an impact on the line shape at $T_0 \simeq 300$ K below 0.1%, a maximum value of ΔT<0.4 K can be estimated from the typical [34] $(T_0/T)^{0.7}$ temperature dependence of the line broadening.

(v) The relative frequency scale should also be precisely known, and the deformation (broadening) by the instrument function should be negligible or precisely modeled, particularly if a conventional Fourier transform spectrometer is used. This issue can be investigated experimentally by using low pressure spectra and analysing both the Doppler broadened profiles of the doublet lines and the spectral distance between them.

(vi) Since the aim is to detect residuals at the level of 0.5 to 1% of the peak absorption, signal to noise ratios of 1000 or more are needed.

(vii) Although some broad pressure-dependent baseline may be included in the fits, the stability of the 100% transmission from one measurement to another is also an important issue.

(viii) From this point of view, introducing a flexibility (e.g. by application of a floated multiplicative factor) in the description of the contribution of “perturbing” lines (weak ones inside the doublet absorption spectral range or those outside of this interval) is also relevant.

(ix) A multispectrum fitting procedure [28], in which a series of spectra recorded in the pressure range defined by (i) are simultaneously adjusted, must imperatively be used in order to minimize the biases associated with correlations among the various floated parameters. Fitting models including and disregarding the SD of LM should be used for comparisons and the results obtained with the hypergeometric and quadratic speed-dependence laws could be analyzed.

(x) Finally, since the perturber mass is expected to have a significant influence (Fig. 6), studying mixtures of NH_3 not only diluted in argon but also in heavier gases (Kr, Xe, SF_6, ..) is of interest.

It is important to remind that, as the fit residuals depend on the weights of the various spectra (e.g. through their number of points) as well as on the spectral range used for the fits, the residuals shown in Figs. 4-7 are only indicative. Those obtained in the treatment of real experiments may have different amplitudes and variations with pressure. It is thus of interest to test the sensitivity of the results to this issue, for instance by removing some points, changing the weights of the various spectra in the multispectrum fits, varying the spectral and/or pressure range(s) retained for the fits.

We are aware that the smallness of the effects that must be detected, with residuals when the SD of LM are disregarded expected to be at the level of one percent or less (see Figs. 4 and 6), together with the numerous measurement constrains discussed above, make devoted experiments very challenging. We however believe that they are worth trying, because the question addressed is, so far, completely open. In parallel, direct theoretical predictions of the speed dependence of all elements of the relaxation matrix (line-broadening, -shifting and -coupling coefficients) based on a reliable NH_3-X intermolecular potential would be of considerable interest. They would enable to better understand the mechanisms involved and could be of great help for the analysis or design of dedicated measurements. Such calculations are not available yet but some approaches do exist (e.g. [35, 36, 37] and those therein) that could be adapted and used for this purpose.

7. Conclusion

Using a realistic theoretical approach, we have investigated the effects of the speed dependence (SD) of line mixing (LM) within NH_3 doublets perturbed by rare gases. This shows that neglecting the SD of LM leads, in the multispectrum fits of a series of spectra calculated for a range of pressures from the Doppler to the strongly overlapping pressure broadened lines regimes, to fit residuals with magnitudes of 0.5 to 1% of the peak absorption. Although a difficult task, highlighting these through experiments seems feasible with modern spectroscopy techniques of high sensitivity and accuracy. With this aim, some guidelines and advices for dedicated measurements have been given which may be of help to experimentalist wishing to tackle the so far unstudied issue of the speed dependence of line mixing.

References

1. Hartmann JM, Boulet C, Robert D.. *Collisional Effects on Molecular Spectra: Laboratory Experiments and Models, Consequences for Applications*. Elsevier, Amsterdam (2008).
2. Hartmann JM, Tran H, Armante R, Boulet C, Campargue A, Forget F, Gianfrani L, Gordon I, Guerlet S, Gustafsson M, Hodges J, Kassi S, Lisak D, Thibault F, Toon G. Recent advances in collisional effects on spectra of molecular gases and their practical consequences. J Quant Spectrosc Radiat Transf 2018;213:178-227.
3. Hartmann JM, Tran H, ,Ngo NH, Landsheere X, Chelin P, Lu X, Liu AW, Hu SM, Gianfrani L, Casa G, Castrillo A, Lepère M, Delière Q, Dhyne M, Fissiaux L. Ab initio calculations of the spectral shapes of CO_2 isolated lines including non-Voigt effects and comparisons with experiments. Phys Rev A 2013;87:013403.
4. Tran H, Ngho NH, Hartmann J-M, Gamache RR, Mondelain D, Kassi S, Campargue A, Gianfrai L, Castrillo A, Fasci E, Rohart F. Velocity effects on the shape of pure H_2O isolated lines: Complementary tests of the partially correlated speed-dependent Keilson-Storer model. J Chem Phys 2013;138:034302.
5. Wehr R, Ciuryło R, Vitcu A, Thibault F, Drummond J.R., May A.D. Dicke-narrowed spectral line shapes of CO in Ar: Experimental results and a revised interpretation. J Mol Spectrosc 2006;235:54-68.
6. Kowzan G, Wcisło P, Słowiński M, Masłowski P, Viel A, Thibault F. Fully quantum calculations of the line-shape parameters for the Hartmann-Tran profile: A CO-Ar case study. J Quant Spectrosc Radiat Transf 2020;243:106803.
7. Nguyen HT, Ngo NH, Tran H. Prediction of line shape parameters and their temperature dependences for CO_2-N_2 using molecular dynamics simulations. J Chem Phys 2018;149:224301.
8. Tran DD, Sironneau VT, Hodges JT, Armante R, Cuesta J, Tran H. Prediction of high-order line-shape parameters for air-broadened O_2 lines using requantized classical molecular dynamics simulations and comparison with measurements. J Quant Spectrosc Radiat Transf 2019;222-223:108-14.
9. Kowzan G, Cybulski H, Wcisło P, Słowiński M, Viel A, Masłowski P, Thibault F. Subpercent agreement between ab initio and experimental collision-induced line shapes of carbon monoxide perturbed by argon. Phys Rev A 2020;102:012821.
10. Słowiński M, Thibault F, Tan Y, Wang J, Liu A, Hu S, Kassi S, Campargue A, Konefał M, Jóźwiak H, Patkowski K, Żuchowski P, Ciuryło R, Lisak D, Wcisło P. H_2-He collisions: Ab initio theory meets cavity-enhanced spectra. Phys Rev A 2020;101:052705.
11. Pine AS. Speed-dependent line mixing in the ν_3 band Q branch of methane. J Quant Spectrosc Radiat Transf 2019;224:62-77.
12. Delahaye T, Ghysels M, Hodges JT, Sung K, Armante R, Tran, H. Measurement and modeling of air□broadened methane absorption in the MERLIN spectral region at low temperatures. J Geophys Res Atmos 2019;124:3556-64.
13. Wilzewski JS, Birk M, Loos J, Wagner G. Temperature-dependence laws of absorption line shape parameters of the CO_2 ν_3 band. J Quant Spectrosc Radiat Transf 2018;206:296-305.
14. Drouin BJ, Benner DC, Brown LR, Cich MJ, Crawford TJ, Malathy Devi V, Guillaume A, Hodges JT, Mlawer EJ, Robichaud DJ, Oyafuso F, Payne VH, Sung K, Wishnow EW, Yu S. Multispectrum analysis of the oxygen A-band. J Quant Spectrosc Radiat Transf 2017;186:118-38.
15. Hadded S, Aroui H, Orphal J, Bouanich JP, Hartmann JM. Line broadening and mixing in NH_3 inversion doublets perturbed by NH_3, He, Ar, and H_2. J Mol Spectrosc 2001;210:275-83.
16. Dhib M, Echargui MA, Aroui H, Orphal J, Hartmann JM. Line shift and mixing in the ν_4 and $2\nu_2$ band of NH_3 perturbed by H_2 and Ar. J Mol Spectrosc 2005;233:138-48.

17. Pine AS, Markov VN. Self- and foreign-gas-broadened lineshapes in the ν_1 band of NH_3. J Mol Spectrosc 2004;228:121-42.
18. Henck SA, Lehmann KK. Coherence transfer between rotation-inversion transitions in the ν_3 fundamental of NH_3. Chem Phys Lett 1988;144:281-5.
19. Starikov VI. Calculation of the relaxation parameters of overlapping lines of the ammonia molecule pressure broadened by argon and helium. Opt Spectrosc 2013;114:15-24.
20. Ma Q, Boulet C, Tipping RH. Relaxation matrix for symmetric tops with inversion symmetry: Line coupling and line mixing effects on NH_3 lines in the ν_4 band. J Chem Phys 2017;146:134312.
21. Berman PR. Speed-dependent collisional width and shift parameters in spectral profiles. J Quant Spectrosc Radiat Transf 1972;12:1331-42.
22. Cherkasov MR. Theory of relaxation parameters of the spectrum shape in the impact approximation−II: Simplifications, application for $^qQ(J,K)$ doublets in the ν_1 band of NH_3 self-broadening. J Quant Spectrosc Radiat Transf 2014;141:89-98.
23. Ciuryło R, Pine AS. Speed-dependent line mixing profiles. J Quant Spectrosc Radiat Transf 2000;67:375-93.
24. Ngo NH, Lisak D, Tran H, Hartmann JM. An isolated line-shape model to go beyond the Voigt profile in spectroscopic databases and radiative transfer codes. J Quant Spectrosc Radiat Transf 2013;129:89-100. Associated Erratum: J Quant Spectrosc Radiat Transf 2014;134:105.
25. Tennyson J, Bernath PF, Campargue A, Csaszar AG, Daumont L, Gamache RR, Hodges JT, Lisak D, Naumenko OV, Rothman LS, Tran H, Zobov NF, Buldyreva J, Boone DC, Hartmann JM, McPheat R, Weidmann D, Murray J, Ngo NH, Polyansky OL. Recommended isolated-line profile for representing high-resolution spectroscopic transitions. Pure Appl Chem 2014;86:1931-43.
26. Rohart F, Mäder H, Nicolaisen HW. Speed dependence of rotational relaxation induced by foreign gas collisions: studies on CH_3F by millimeter coherent transients. J Chem Phys 1994;101:6475-86.
27. Gordon IE, Rothman LS, Hill C, Kochanov RV, Tan Y, Bernath PF, Birk M, Boudon V, Campargue A, Chance KV, Drouin BJ, Flaud JM, Gamache RR, Hodges JT, Jacquemart D, Perevalov VI, Perrin A, Shine KP, Smith MAH, Tennyson J, Toon GC, Tran H, Tyuterev VG, Barbe A, Császár AG, Devi VM, Furtenbacher T, Harrison JJ, Hartmann JM, Jolly A, Johnson TJ, Karman T, Kleiner I, Kyuberis AA, Loos J, Lyulin OM, Massie ST, Mikhailenko SN, Moazzen-Ahmadi N, Müller HSP, Naumenko OV, Nikitin AV, Polyansky OL, Rey M, Rotger M, Sharpe SW, Sung K, Starikova E, Tashkun SA, Vander Auwera J, Wagner G, Wilzewski J, Wcisło P, Yu S, Zak EJ. The HITRAN2016 Molecular Spectroscopic Database. J Quant Spectrosc Radiat Transf 2017;203:3-69
28. Benner DC, Rinsland CP, Malathy Devi V, Smith MAH, Atkins D. A multispectrum nonlinear least squares fitting technique. J Quant Spectrosc Radiat Transf 1995;53:705-21.
29. Tran H, Hartmann JM, Toon G, Brown LR, Frankenberg C, Warneke T, Spietz P, Hase F. The $2\nu_3$ band of CH_4 revisited with line mixing: Consequences for spectroscopy and atmospheric retrievals at 1.67μm. J Quant Spectrosc Radiat Transf 2010;111:1344-56.
30. Ngo NH, Lin H, Hodges JT, Tran H. Spectral shapes of rovibrational lines of CO broadened by He, Ar, Kr and SF_6: A test case of the Hartmann-Tran profile. J Quant Spectrosc Radiat Transf 2017;203:325-33.
31. Ngo NH, Hartmann JM. A strategy to complete databases with parameters of refined line shapes and its test for CO in He, Ar and Kr. J Quant Spectrosc Radiat Transf 2017;203:334-40.
32. Lisak D, CyganA, Bermejo D, Domenech JL, Hodges JT, Tran H. Application of the Hartmann-Tran profile to analysis of H_2O spectra. J Quant Spectrosc Radiat Transf 2015;164:221-30.
33. Gupta V, Rohart F, Margulès L, Motiyenko RA, Buldyreva J. Line-shapes and broadenings of rotational transitions of $CH_3{}^{35}Cl$ in collision with He, Ar and Kr. J Quant Spectrosc Radiat Transf 2015;161:85-94.

34. Sur R, Spearrin RM, Peng WY, Strand CL, Jeffries JB, Enns GM, Hanson RK. Line intensities and temperature-dependent line broadening coefficients of Q-branch transitions in the ν_2 band of ammonia near 10.4 μm. J Quant Spectrosc Radiat Transf 2016;175:90-9.
35. Wang WF. Theoretical study of quantum scattering cross-sections and second-virial coefficients of NH_3–He using a recent potential energy surface. Chem Phys 2003;288:23-31.
36. Bouhafs N, Rist C, Daniel F, Dumouchel F, Lique F, Wiesenfeld L, Faure A. Collisional excitation of NH_3 by atomic and molecular hydrogen, Mon Not Roy Astron Soc 2017;470:2204-11.
37. Van der Sanden GCM, Wormer PES, van der Avoird A. Differential cross sections for rotational excitation of NH_3 by collisions with Ar and He: Close coupling results and comparison with experiment. J Chem Phys 1996;105:3079-88.